The EMBO Journal Vol.19 No.3 pp.421–433, 2000

The Bbp1p–Mps2p complex connects the SPB to the nuclear envelope and is essential for SPB duplication

Carolin Schramm, Sarah Elliott, Anna Shevchenko[1], Andrej Shevchenko[1] and Elmar Schiebel[2]

The Beatson Institute for Cancer Research, CRC Beatson Laboratories, Glasgow G61 1BD, UK and [1]Peptide and Protein Group, European Molecular Biology Laboratory (EMBL), Meyerhofstraße 1, 69012 Heidelberg, Germany

[2]Corresponding author
e-mail: eschiebe@udcf.gla.ac.uk

In budding yeast, microtubules are organized by the spindle pole body (SPB), which is embedded in the nuclear envelope via its central plaque structure. Here, we describe the identification of *BBP1* in a suppressor screen with a conditional lethal allele of *SPC29*. Bbp1p was detected at the central plaque periphery of the SPB and *bbp1-1* cells were found to be defective in SPB duplication. *bbp1-1* cells extend their satellite into a duplication plaque like wild-type cells; however, this duplication plaque then fails to insert properly into the nuclear envelope and does not assemble a functional inner plaque. This function in SPB duplication is probably fulfilled by a stable complex of Bbp1p and Mps2p, a nuclear envelope protein that is also essential for duplication plaque insertion. In addition, we found that Bbp1p interacts with Spc29p and the half-bridge component Kar1p. These interactions are likely to play a role in connecting the SPB with the nuclear envelope and the central plaque with the half-bridge.

Keywords: Bbp1p/Kar1p/Mps2p/SPB duplication/Spc29p

Introduction

In budding yeast, microtubule organizing functions are provided by the spindle pole body (SPB), a multi-layered structure that is embedded in the nuclear envelope throughout the cell cycle (Byers and Goetsch, 1975). SPB substructures named the outer, central and inner plaque and the half-bridge have been described by electron microscopy. The central plaque plays a role in embedding the SPB into the nuclear envelope, whereas the outer and inner plaques function in cytoplasmic and nuclear microtubule organization, respectively. The half-bridge, a one-sided extension of the central plaque, is essential for the cell-cycle-dependent duplication of the SPB and in addition it organizes cytoplasmic microtubules (Byers and Goetsch, 1975; Brachat *et al.*, 1998; Pereira *et al.*, 1999).

The central plaque contains a two-dimensional crystal formed by the SPB component Spc42p (Bullitt *et al.*, 1997). The Tub4p complex binding protein Spc110p is anchored to the nuclear side of this Spc42p layer via Spc29p, which interacts with the N-terminal domain of Spc42p and a C-terminal portion of Spc110p (Knop and Schiebel, 1997; Elliott *et al.*, 1999). Towards the cytoplasmic side, Spc42p binds to Cnm67p (Brachat *et al.*, 1998; Wigge *et al.*, 1998; Adams and Kilmartin, 1999; Elliott *et al.*, 1999).

In early G_1 phase of the cell cycle the cytoplasmic side of the half-bridge develops the satellite at its most distal end (Byers and Goetsch, 1975). The satellite contains the central/outer plaque components Spc29p, Spc42p, Cnm67p and Nud1p (Adams and Kilmartin, 1999), suggesting that it is a miniature version of the central/outer plaque of the SPB. After Start of the cell cycle the satellite extends into a duplication plaque, which is then inserted into the nuclear envelope (Byers and Goetsch, 1975; Adams and Kilmartin, 1999). In contrast, the inner plaque containing Spc110p/calmodulin and the Tub4p complex, is most likely to assemble within the nucleus (Pereira *et al.*, 1998; Adams and Kilmartin, 1999; Elliott *et al.*, 1999) and is attached to the central/outer plaque via the binding of Spc110p to Spc29p (Elliott *et al.*, 1999).

CDC31 and *KAR1* function in SPB duplication before Start of the cell cycle (Baum *et al.*, 1986; Rose and Fink, 1987). In contrast, *MPS1*, *MPS2*, *NDC1* and *SPC29* play a role in SPB duplication after Start (Winey *et al.*, 1991, 1993; Biggins *et al.*, 1996; Chial *et al.*, 1998; Adams and Kilmartin, 1999; de la Cruz Munoz-Centeno *et al.*, 1999; Elliott *et al.*, 1999). The yeast centrin Cdc31p and Kar1p are interacting components of the half-bridge (Spang *et al.*, 1993, 1995; Biggins and Rose, 1994). The dual specific kinase Mps1p functions in SPB duplication and in mitotic check point control (Lauzé *et al.*, 1995; Weiss and Winey, 1996). *NDC1* and *MPS2* encode nuclear envelope proteins that are associated with the region of the central plaque that is in contact with the nuclear envelope (Chial *et al.*, 1998; de la Cruz Munoz-Centeno *et al.*, 1999) and the encoded proteins facilitate the insertion of the duplication plaque into the nuclear envelope (Winey *et al.*, 1991, 1993; Chial *et al.*, 1998; de la Cruz Munoz-Centeno *et al.*, 1999). The SPB duplication function of Spc29p is probably fulfilled by the fraction of the protein that is associated with the satellite (Adams and Kilmartin, 1999).

To understand the function of *SPC29* further we performed a high gene dosage suppressor screen, which identified *BBP1*, encoding an essential SPB component (Wigge *et al.*, 1998), as a suppressor of the temperature-sensitive growth defect of *spc29(ts)* cells. We show that Bbp1p interacts with Spc29p, the nuclear envelope protein Mps2p and the half-bridge component Kar1p. These multiple interactions of Bbp1p are probably important for the insertion of the duplication plaque into the nuclear envelope during SPB duplication as well as for connecting the half-bridge with the central plaque.

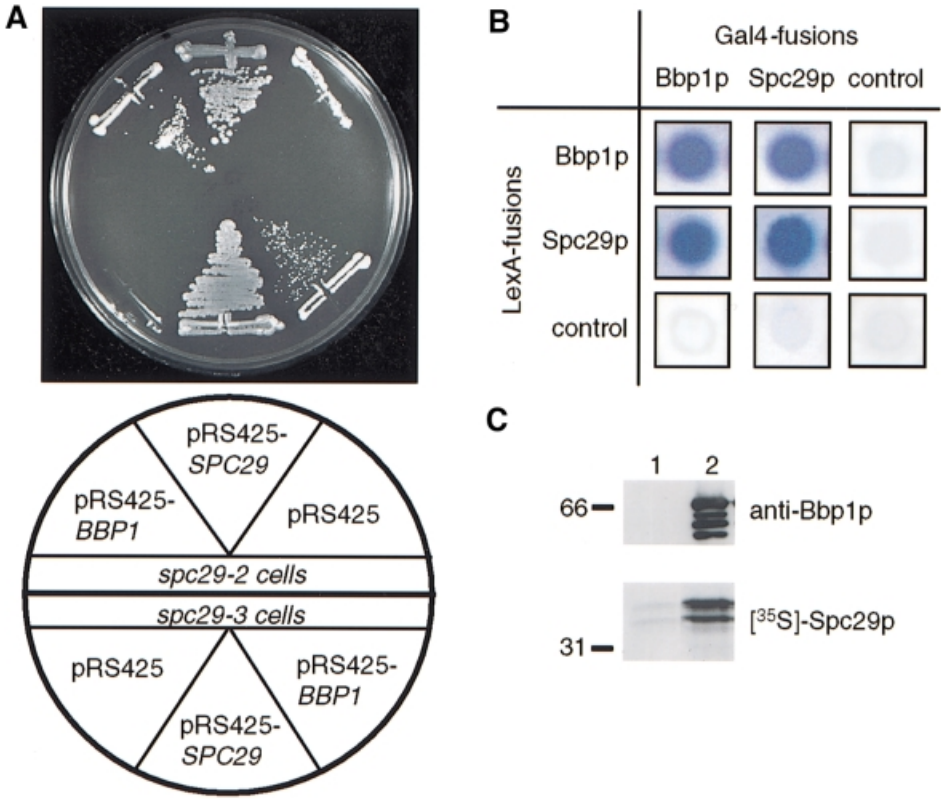

Fig. 1. Bbp1p interacts with Spc29p. (**A**) *BBP1* is a high gene dosage suppressor of the temperature-dependent growth defect of *spc29(ts)* cells. Cells of *spc29-2* and *spc29-3* with the indicated plasmids were incubated for 3 days at 35°C. (**B**) Two-hybrid interactions between Spc29p and Bbp1p. Blue colony colour indicates interaction. The control cells carry e.g. the pMM5 derived *LexA-BBP1* plasmid combined with pMM6 without insert. (**C**) Binding of Spc29p to Bbp1p. ^{35}S-labelled Spc29p was incubated with purified GST (lane 1) or GST–Bbp1p (lane 2) bound to glutathione–Sepharose beads. The bound proteins were eluted and analysed by immunoblotting with anti-Bbp1p antibodies or by autoradiography ([^{35}S]Spc29p).

Results

BBP1 interacts with SPC29

To get a better understanding of the role of *SPC29* in SPB duplication (Adams and Kilmartin, 1999; Elliott *et al.*, 1999), we searched for high gene dosage suppressors of the temperature-dependent growth defect of conditional lethal *spc29(ts)* cells. *CDC31*, which functions in SPB duplication (Baum *et al.*, 1986), was identified as a high gene dosage suppressor of the *spc29-2* allele; however, it did not allow cells of *spc29-3* to grow at the restrictive temperature (Elliott *et al.*, 1999). *BBP1* was found as an additional suppressor of the temperature-dependent growth defect of *spc29-2* and of *spc29-3* cells (Figure 1A). Since *BBP1* and *SPC29* code for SPB components (Wigge *et al.*, 1998), their genetic interaction raised the possibility that the two proteins bind to each other. Support for this comes from the finding that Bbp1p and Spc29p interacted in the yeast two-hybrid system (Figure 1B). In addition, we observed that *SPC29* or *BBP1* combined with themselves showed two-hybrid interactions, suggesting that they form homodimers or homomultimers. No signal was observed when the *BBP1*- and *SPC29*-containing plasmids were combined with vector controls (Figure 1B).

Attempts to co-immunoprecipitate Bbp1p and Spc29p failed. This may reflect the strong binding of Spc29p to Spc42p and Spc110p (Elliott *et al.*, 1999) and of Bbp1p to Mps2p (see below). The weaker interaction between Bbp1p and Spc29p may, therefore, be disrupted upon salt extraction of SPBs. To confirm the binding of Spc29p to Bbp1p we performed an *in vitro* binding experiment. *In vitro* translated Spc29p was incubated with recombinant, purified glutathione *S*-transferase (GST)–Bbp1p fusion protein (Figure 1C, lane 2, anti-Bbp1p blot) or with GST. The latter exceeded the amount of GST–Bbp1p by at least a factor of 3–5 (data not shown). Spc29p bound strongly to GST–Bbp1p (Figure 1C, lane 2; [^{35}S]Spc29p) but hardly to GST beads (lane 1), suggesting a direct interaction of Spc29p with Bbp1p. Taken together, Spc29p binds directly to Bbp1p.

Bbp1p is associated with the periphery of the central plaque

We determined the localization of Bbp1p within the SPB by immunoelectron microscopy using affinity-purified antibodies that specifically recognize Bbp1p (Figure 2A) or the fully functional epitope-tagged Bbp1p-3Myc derivative. Secondary antibodies were either coupled to ultrasmall gold particles to allow penetration inside SPB substructures (Figure 2B and C; Adams and Kilmartin, 1999) or to 12 nm gold particles (Figure 2D). Using yeast cells, we observed a Bbp1p-3Myc signal close to the central plaque periphery ($n = 10$) (Figure 2B, arrow), frequently towards the cytoplasmic side of the SPB. When isolated nuclei were used the gold particles were also found near the periphery of the central plaque ($n = 20$) (Figure 2C, middle panel). In cases in which a half-bridge was visible ($n = 3$), the anti-Bbp1p signal was close to the site where the half-bridge touched the central plaque

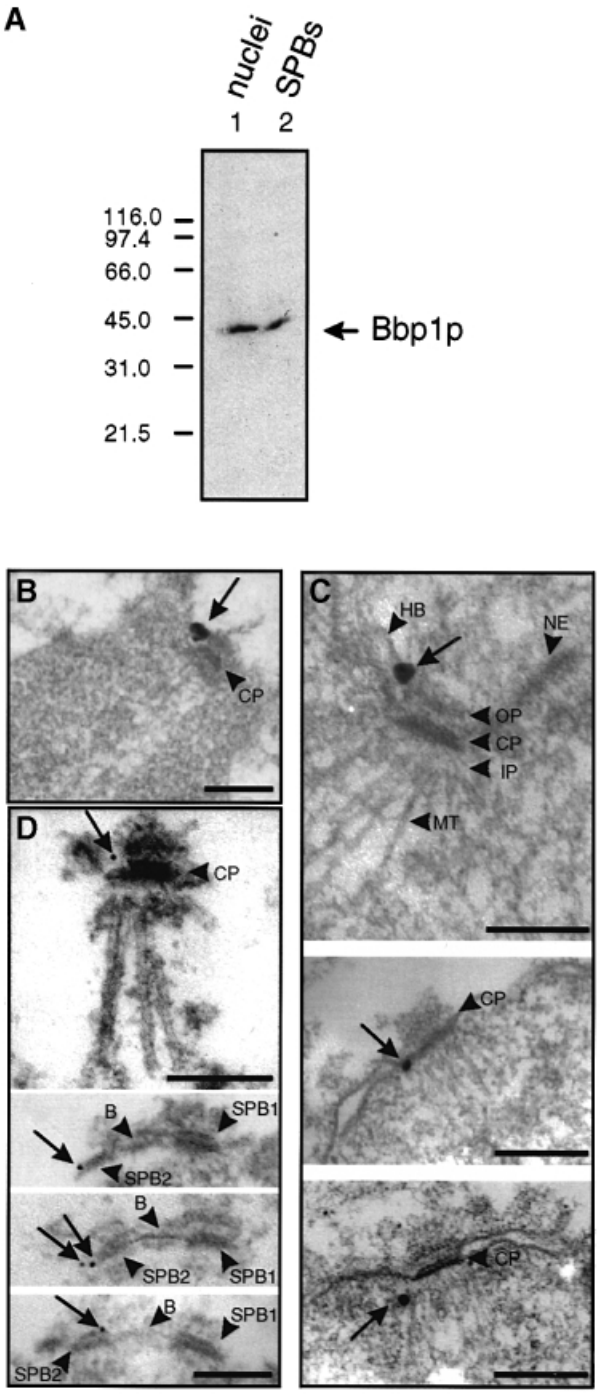

Fig. 2. Bbp1p is associated with the central plaque periphery. (**A**) The anti-Bbp1p antibodies recognize specifically Bbp1p. Enriched nuclei (lane 1) or SPBs (lane 2) were probed with affinity-purified anti-Bbp1p antibodies. (**B–D**) Bbp1p is located close to the periphery of the central plaque (see arrows). (B) *BBP1-3Myc* cells were labelled with anti-Myc antibodies. (C) Enriched nuclei or (D) isolated SPBs of wild-type cells were incubated with affinity-purified anti-Bbp1p antibodies. (B and C) The secondary antibodies were conjugated with ultrasmall gold particles, which were silver enhanced. (D) The secondary antibodies were conjugated with 12 nm gold particles. Note that the duplicated SPBs (SPB1 and SPB2) in the bottom half of (D) are still connected via the bridge structure. B, bridge; CP, central plaque; HB, half-bridge; IP, inner plaque; MT, microtubule; NE, nuclear envelope; OP, outer plaque. Bars (B–D), 0.25 μm.

periphery (Figure 2C, top panel). In a few cases ($n = 2$) the anti-Bbp1p signal was located near the inner plaque of the SPB (Figure 2C, lower panel). This may either indicate a second localization of Bbp1p within the SPB or reflect the fact that Bbp1p is connected to the gold particles via the primary and secondary antibodies. The localization of Bbp1p with the central plaque periphery was further confirmed using isolated SPBs ($n = 40$) (Figure 2D, top panel, arrow). When two side-by-side SPBs connected via the bridge structure were observed ($n = 5$), the Bbp1p signal was located either next to the site where the bridge touched the central plaque (Figure 2D, bottom) or at the central plaque periphery opposite to this bridge attachment side (Figure 2D, middle). Thus, Bbp1p is located near the central plaque periphery of the SPB.

BBP1 is essential for proper SPB duplication

The function of Bbp1p at the SPB was investigated by analysing the phenotype of conditional lethal *bbp1(ts)* mutants. Growth of wild-type and *bbp1-1* cells was arrested with α-factor at 23°C, the permissive temperature of *bbp1-1* cells, in the G_1 phase of the cell cycle. These cells continued synchronously in the cell cycle when α-factor was removed by washing the cells (Figure 3A, $t = 0$). Simultaneously, the cells were shifted to 37°C, the restrictive temperature of *bbp1-1* cells. After 1.5 h wild-type cells had replicated their chromosomes (Figure 3A), had duplicated the SPB (Figure 3B-1 and B-2) and finally formed a mitotic spindle, which segregated the chromosomes, indicated by the two DAPI-staining regions in the mother cell body and the bud (Figure 3B-1 and B-2, DAPI; note that the mother cell body is still associated with the mating projection). Wild-type cells then exited mitosis and continued their progression through the cell cycle (Figure 3A). Cells of *bbp1-1* also replicated their DNA; however, 1.5 h after the temperature shift these cells arrested temporarily with a 2*n* chromosome content and a large bud with only one DAPI-staining region in the bud neck (Figure 3A, B-3–B-6; Table I). Anti-tubulin staining revealed that 99% of the large budded *bbp1-1* cells failed to form a proper mitotic spindle (Table I), explaining the defect in chromosome segregation. Several spindle defects were observed. About 40% of large budded *bbp1-1* cells contained only one signal when antibodies against the outer plaque protein Spc72p were used (Figure 3B-3; Table I), suggesting an SPB duplication or separation defect in these cells. The remainder (Figure 3B-4–B-6) had two anti-Spc72p signals and in most of the cases a strong nuclear microtubule bundle originated from only one SPB, whereas the other SPB was associated with none or only a few nuclear microtubules (Figure 3B-5 and B-6, arrow). The latter SPB was non-functional in chromosome segregation because the DAPI-staining region was associated with the SPB that organized the extended nuclear microtubule bundle. Other large budded *bbp1-1* cells (14%) contained what looked like a bipolar spindle (Figure 3B-4). However, only the SPB in the mother cell body was associated with a DAPI-staining region, suggesting that the nuclear microtubules organized by the other SPB were not functional. Furthermore, the nuclear microtubule bundle associated with the non-functional SPB were clearly thinner compared with the bundle originating from the functional SPB. Both SPBs of

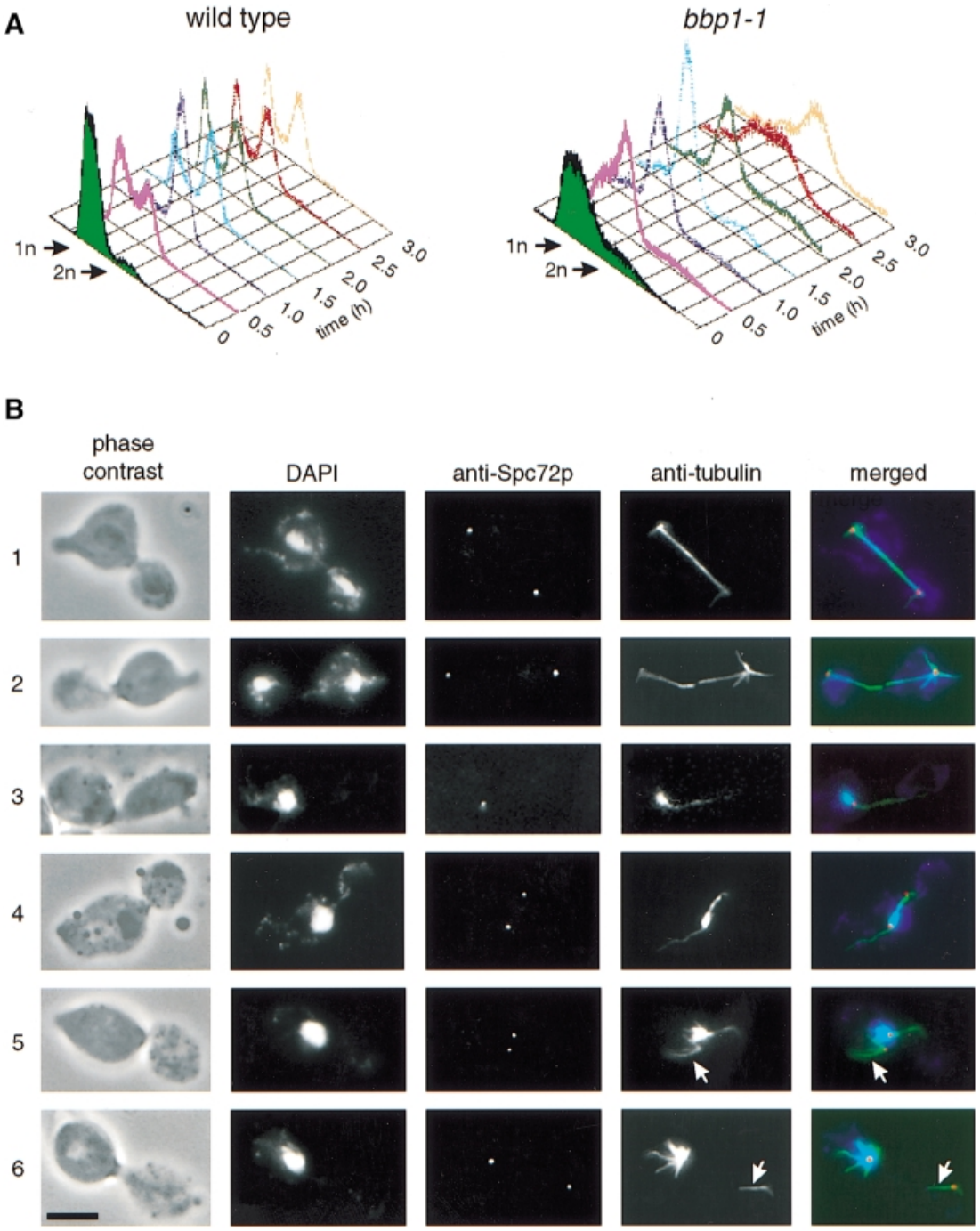

Fig. 3. Cells of *bbp1-1* are defective in mitotic spindle formation and chromosome segregation. Wild-type and *bbp1-1* cells were synchronized with α-factor in the G_1 phase of the cell cycle. α-factor was removed by washing the cells ($t = 0$). Simultaneously, the cells were shifted to 37°C, the restrictive temperature. (**A**) The DNA content of wild-type and *bbp1-1* cells was followed over time by flow cytometry. (**B**) Fixed wild-type (B-1 and B-2) and *bbp1-1* cells (B-3–B-6) were analysed by indirect immunofluorescence microscopy with affinity-purified rabbit anti-Spc72p antibodies and mouse monoclonal anti-tubulin antibodies 1.5 h after the temperature shift. DNA was stained with DAPI. The anti-Spc72p (red), anti-tubulin (green) and DAPI (blue) signals were merged. Cells were also inspected by phase-contrast microscopy. Bar, 5 μm.

bbp1-1 cells were frequently associated with cytoplasmic microtubules, which probably assisted the positioning of the nucleus in the bud neck region of the large budded cell.

The failure of one SPB of *bbp1-1* cells to organize functional nuclear microtubules suggests that this SPB is defective. To identify the SPB defect, a synchronized culture of *bbp1-1* cells was shifted to the restrictive temperature and the morphology of the SPBs and the spindle was followed over time by electron microscopy. One hour after the temperature shift cells of *bbp1-1* ($n = 20$) had enlarged their satellite into a duplication plaque (Figure 4A; five different SPBs with duplication plaques connected to the half-bridge are shown), which was similar in appearance to that observed for wild-type cells (Adams and Kilmartin, 1999)

Table I. Phenotypic analysis of synchronized *bbp1-1* cells

	time in h							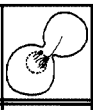		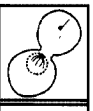
wild type	0	100	0	0	0	0	0	0	0	0
	0.5	25	70	5	0	0	0	0	0	0
	1.0	1	30	38	31	0	0	0	0	0
	1.5	30	3	2	60	5	0	0	0	0
bbp1-1	0	100	0	0	0	0	0	0	0	0
	0.5	18	82	0	0	0	0	0	0	0
	1.0	2	21	0	2	0	31	16	8	20
	1.5	0	0	0	1	0	40	2	14	43

Wild-type and *bbp1-1* cells were synchronized with α-factor and shifted to 37°C as described in the legend to Figure 3. Cells were fixed with formaldehyde for 1 h and analysed by indirect immunofluorescence using rabbit anti-Spc72p and mouse anti-tubulin antibodies. DNA was stained with DAPI. About 200 cells were counted per time point. The SPB is indicated as a dot. The DAPI staining region is drawn as a dotted circle. Values given as percentages.

(data not shown). In all 20 inspected wild-type cells this duplication plaque was inserted into the nuclear envelope (Figure 4B, SPB2) ~1.25 h after the cell cycle release and gained the nuclear inner plaque with nuclear microtubules (Figure 4B, two consecutive sections through a wild-type cell are shown; note the nuclear microtubules associated with the new SPB2). In contrast, the duplication plaque of *bbp1-1* cells was not inserted into the nuclear envelope after 1.25 h ($n = 25$) (Figure 4C, two sections through a *bbp1-1* cell are shown; note the absence of nuclear microtubules associated with the duplication plaque, here designated SPB2), suggesting that this step is delayed or defective in *bbp1-1* cells. As reported previously (Adams and Kilmartin, 1999), a nuclear pore was frequently associated with the duplication plaque (Figure 4C). After 1.5 h only one normal looking SPB was observed in most serial sections through whole *bbp1-1* cells ($n = 50$), despite the appearance of two anti-Spc72p signals in 63% of *bbp1-1* cells. This may be explained by a partial disintegration of the newly formed SPB structure, a phenotype that has been described for some *spc29(ts)* and *spc110(ts)* mutants (Sundberg and Davis, 1997; Adams and Kilmartin, 1999). Alternatively, the defective SPB of *bbp1-1* cells may not be recognized as such because its appearance by electron microscopy may be similar to nuclear pores, in particular when no nuclear microtubules were organized. However, two examples of *bbp1-1* cells with two SPBs were observed by electron microscopy after 1.5 h at 37°C (Figure 4D and E, each shows two serial sections through a *bbp1-1* cell). One SPB was smaller (Figure 4D and E, SPB2) compared with the other wild-type-looking SPB (SPB1), and the smaller SPB was associated with hardly any (Figure 4D) or only a few nuclear microtubules (Figure 4E). In contrast to wild-type cells (Figure 4F, four sections through a wild-type cell are shown) these *bbp1-1* cells failed to form a bipolar spindle. Instead, the few nuclear microtubules organized by the smaller SPB failed to connect the nuclear microtubules of the other SPB (Figure 4E). Similar results were obtained with *bbp1-2* cells (data not shown).

The observation that some of the defective SPBs of *bbp1-1* cells organize nuclear microtubules suggests that at least in these cases the duplication plaque was inserted into the nuclear envelope, followed by the assembly of the nuclear inner plaque. This possibility was tested by constructing *bbp1-1* cells that expressed *SPC42-GFP* or *SPC110-GFP* gene fusions. Spc42p is associated with the cytoplasmic central plaque as well as with the duplication plaque (Adams and Kilmartin, 1999; Elliott *et al.*, 1999). Spc110p is a component of the nuclear inner plaque that assembles into the SPB from the nucleus (Rout and Kilmartin, 1990; Kilmartin and Goh, 1996) after the duplication plaque was inserted into the nuclear envelope (Adams and Kilmartin, 1999). We compared the number of Spc42p and Spc110p signals in large budded *bbp1-1* cells. Similarly to the indirect immunofluorescence experiment using the outer plaque protein Spc72p as a marker (Table I), 54% of large budded *bbp1-1* cells showed two Spc42p signals when incubated at 37°C for 1.5 h (Figure 5B). In contrast only 16% of *bbp1-1* cells contained two Spc110p signals (Figure 5A). Therefore, in *bbp1-1* cells only about one-third of the newly formed SPBs that form an outer plaque also assemble an inner plaque.

Taken together, *bbp1-1* cells are defective in proper SPB duplication such that most *bbp1-1* cells fail to assemble a nuclear inner plaque. In the cases in which *bbp1-1* cells managed to form an inner plaque very few nuclear microtubules were organized and these proved to be non-functional.

Bbp1p functions together with the integral membrane protein Mps2p

To identify proteins that interact with Bbp1p, Bbp1p-containing complexes were purified from a strain that carried a functional gene fusion of *BBP1* and protein A (*BBP1–ProA*). Bbp1p–ProA was enriched using IgG–Sepharose to which protein A binds with high affinity (Knop and Schiebel, 1997). After several washing steps, proteins with apparent mol. wts of 45, 46 and 60 kDa were eluted from the IgG resin (Figure 6A, lane 2). The binding of these proteins was dependent on the expression of *BBP1–ProA*, since they were not among the proteins of *BBP1* cells that bound non-specifically to IgG–Sepharose (Figure 6A, lane 1). These proteins were analysed by mass spectroscopy (Shevchenko *et al.*, 1996). The 60 kDa

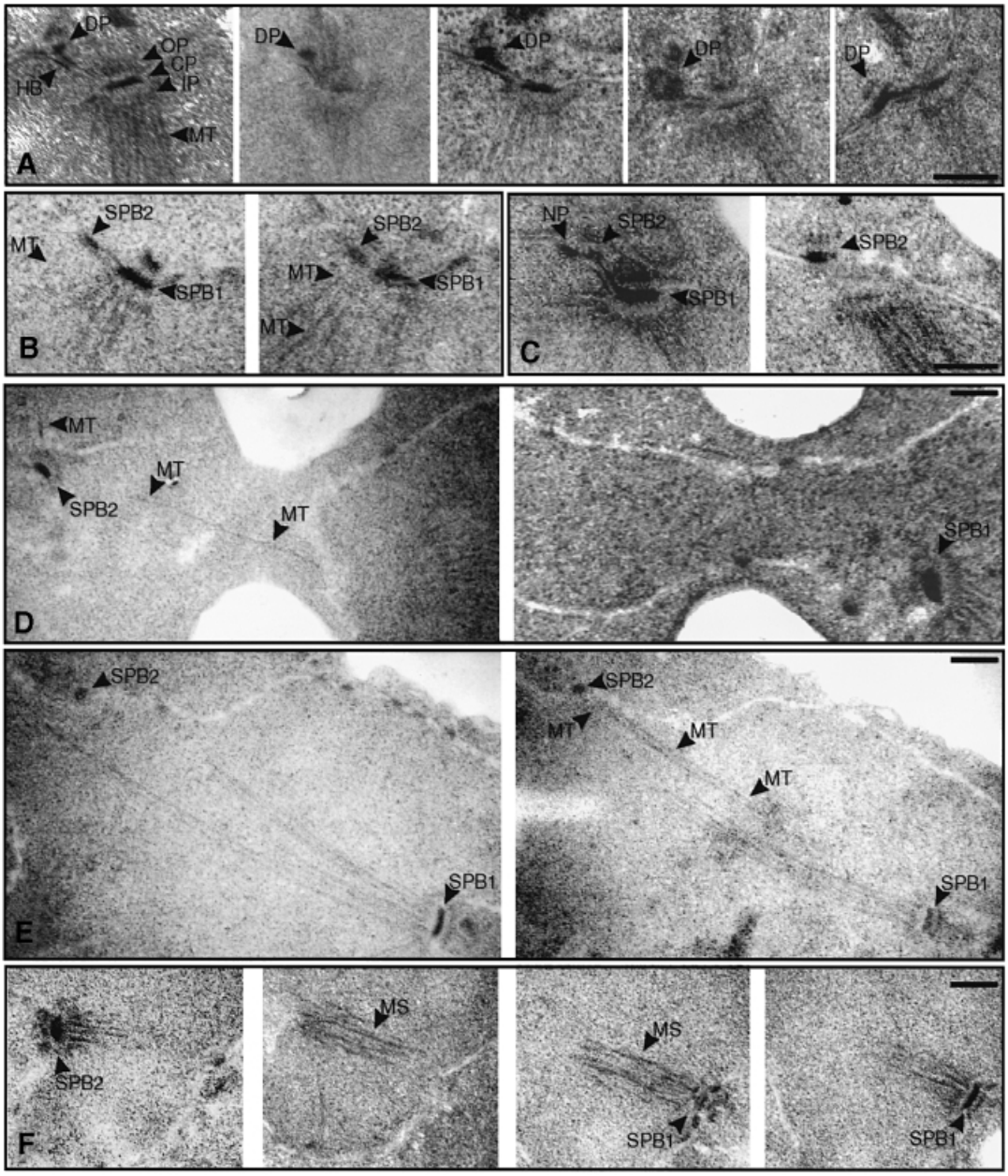

Fig. 4. Proper insertion of the duplication plaque into the nuclear envelope is defective in *bbp1-1* cells. Synchronized wild-type and *bbp1-1* cells (see the legend to Figure 3) were prepared for thin-section electron microscopy 1, 1.25 and 1.5 h after they had been shifted from 23 to 37°C ($t = 0$). Serial sections which span the entire nucleus were analysed. (**A**) Five sections through different *bbp1-1* cells (1 h at 37°C) are shown. The mother SPB consists of an outer, central and inner plaque. The duplication plaque (DP) is associated with the distal tip of the half-bridge. (**B**) Two serial sections through a wild-type cell 1.25 h after the temperature shift. The former duplication plaque (SPB2) is now inserted in the nuclear envelope and has assembled an inner plaque with associated nuclear microtubules (MT). (**C**) Two serial sections through a *bbp1-1* cell (1.25 h). The duplication plaque (named SPB2) is not inserted in the nuclear envelope. Nuclear microtubules are not associated with the duplication plaque in any of the serial sections. As reported before (Adams and Kilmartin, 1999), a nuclear pore (NP) was often observed close to the duplication plaque. (**D** and **E**) Two serial sections through two nuclei of *bbp1-1* cells (1.5 h). One SPB (SPB1) appears similar as in wild-type cells, whereas the other (SPB2) is smaller and associated with fewer nuclear microtubules (MT). (**F**) Four consecutive serial sections through a wild-type cell (1.5 h). The two SPBs (SPB1 and SPB2) form a mitotic spindle (MS). CP, central plaque; DP, duplication plaque; HB, half-bridge; IP, inner plaque; MS, mitotic spindle; MT, microtubules; NP, nuclear pore; OP, outer plaque. Bars (A–F), 0.25 μm.

band was identified as Bbp1p–ProA (data not shown), whereas the 45/46 kDa doublet is encoded by *MPS2* (Figure 6B). *MPS2* functions in SPB duplication (Winey *et al.*, 1991) and the encoded protein is associated with the nuclear envelope and the SPB periphery (de la Cruz Munoz-Centeno *et al.*, 1999).

The interaction of Bbp1p and Mps2p was verified by an immunoprecipitation experiment. Extracts of yeast cells expressing either *MPS2 BBP1-3Myc* (Figure 6C, lanes 1 and 3) or *MPS2-3HA BBP1-3Myc* (lanes 2 and 4) were used. These extracts were incubated with anti-hemagglutinin (HA) (12CA5) antibodies coupled to protein A–Sepharose beads, followed by analysis of the precipitated proteins by immunoblotting with anti-HA (Figure 6C, lanes 5 and 6) and anti-Myc antibodies (lanes 7 and 8). The immunoblots revealed that Bbp1p–3Myc

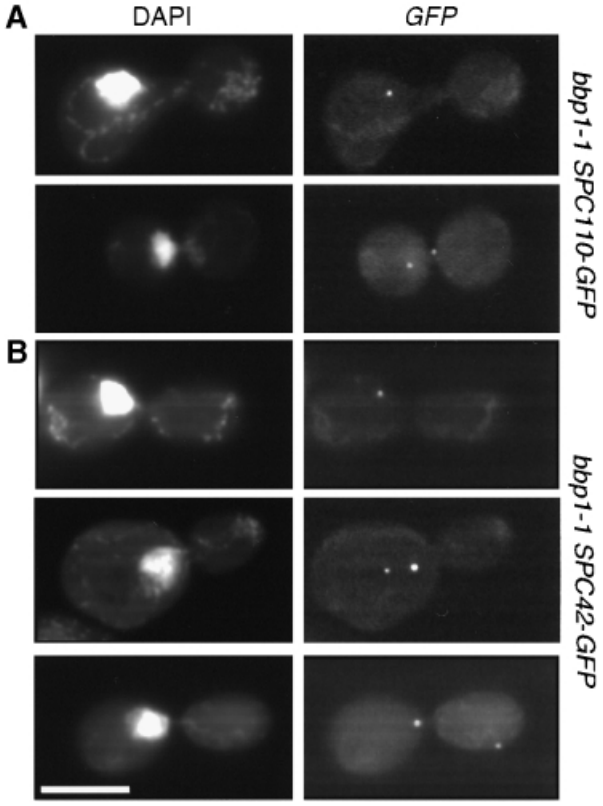

Fig. 5. Many *bbp1-1* cells fail to assemble a nuclear inner plaque. α-factor-synchronized *bbp1-1* cells containing (**A**) *SPC110-GFP* or (**B**) *SPC42-GFP* were shifted to the restrictive temperature for 1.5 h. Cells were fixed with paraformaldehyde and DNA was stained with DAPI. Approximately half of large budded *bbp1-1 SPC42-GFP* cells (54%) carried two SPB signals. Only 16% of *bbp1-1 SPC110-GFP* cells with two SPB signals were detected. Bar, 5 μm.

(Figure 6C, lane 8) was co-immunoprecipitated with Mps2p–3HA (lane 6). This precipitation was specific, since it was not observed when the *MPS2 BBP1–3Myc* cell extract was used (Figure 6C, lanes 5 and 7). Similarly, Mps2p–3Myc was co-immunoprecipitated with Bbp1p–3HA but not with Bbp1p using anti-HA antibodies (data not shown). These results suggest that Bbp1p and Mps2p are part of common complexes.

A functional interaction of *BBP1* and *MPS2* is further suggested by their genetic interaction. *MPS2* was found to be a high gene dosage suppressor of the temperature-dependent growth defect of *bbp1-1* cells (Figure 6D-1). Furthermore, *BBP1* on a 2 μm plasmid allowed *mps2-2* (Figure 6D-2) and *mps2-42* cells (data not shown), but not *mps2-1* cells (Figure 6D-3), to grow at the restrictive temperature. In addition, Bbp1p interacted with Mps2p in the yeast two-hybrid system (Figure 6E). We also noticed that Mps2p combined with itself gave a signal. Taken together, Bbp1p and Mps2p function together in common complexes.

Bbp1p binds directly to Mps2p

Using an *in vitro* binding assay, we investigated whether bacterial expressed Bbp1p and Mps2p interact directly. The purified His_6-$Mps2p^{1–307}$ (Figure 7A, lane 2), lacking the membrane-spanning region, bound to immobilized GST–Bbp1p (lane 3), but not to GST (Figure 7A, compare lanes 8 and 9). Furthermore, we observed that His_6-$Mps2p^{1–307}$ interacted with similar efficiency with the C-terminal portion of $Bbp1p^{202–385}$ (lanes 4 and 5) as with full-length Bbp1p (compare lanes 3 and 5). When His_6-$Mps2p^{1–307}$ was incubated with the N-terminal part of Bbp1p a faint protein band corresponding in size to His_6-$Mps2p^{1–307}$ was observed in some experiments (Figure 7A, lane 7, asterisk). However, this band was not recognized by the anti-His tag antibodies (Figure 7C, lane 7). It may represent a Bbp1p degradation product. Alternatively, His_6-$Mps2p^{1–307}$ may bind weakly to the N-terminal part of Bbp1p, but the low amount of His_6-$Mps2p^{1–307}$ was not detected by the anti-His tag antibodies, which recognized His_6-$Mps2p^{1–307}$ rather poorly. The identity of the GST- (Figure 7B) and His_6-tagged (Figure 7C) fusion proteins was confirmed by immunoblotting. Taken together, the C-terminal half of Bbp1p interacts directly with Mps2p.

BBP1 interacts with KAR1

Our data are consistent with a model in which a complex containing Bbp1p and Mps2p is associated with the central plaque periphery. Since the half-bridge is connected with the central plaque (Byers and Goetsch, 1975), Bbp1p or Mps2p may also interact with components of the half-bridge. The two known components of the half-bridge are encoded by *CDC31* and *KAR1* (Vallen *et al.*, 1992; Spang *et al.*, 1993, 1995). We found that *KAR1*, on a centromere-based plasmid, increased the growth defect of *bbp1-1* (Figure 8A) but not of *mps2-2* cells (data not shown). Such an effect of *KAR1* has been described for *CDC31* (Vallen *et al.*, 1994) and *SPC29* (Elliott *et al.*, 1999) mutant cells, both of which are defective in SPB duplication (Baum *et al.*, 1986; Adams and Kilmartin, 1999; Elliott *et al.*, 1999). In addition, Bbp1p interacted with Kar1p (Figure 8B), but not with Cdc31p (data not shown), in the yeast two-hybrid system. As descibed for other two-hybrid interactions (Knop and Schiebel, 1997, 1998), the Bbp1p–Kar1p interaction was only detectable in the indicated combination, but not when *LexA–KAR1* and *GAL4–BBP1* were combined (data not shown). Considering that Bbp1p is located close to the site where the half-bridge touches the central plaque (Figure 2), it is possible that Bbp1p is involved in connecting the central plaque with the half-bridge.

Discussion

Bbp1p interacts with Mps2p and Spc29p

In this study we identified *BBP1*, coding for an essential SPB protein (Wigge *et al.*, 1998), as a suppressor of the temperature-dependent growth defect of *spc29-2* and *spc29-3* cells. The genetic interaction of *BBP1* with *SPC29* raised questions regarding the function of Bbp1p and in particular its relationship to Spc29p and to other proteins involved in SPB duplication.

Bbp1p was found to interact with Spc29p in the yeast two-hybrid system and *in vitro* translated Spc29p bound directly to recombinant GST–Bbp1p. This, together with the genetic interaction of *BBP1* and *SPC29*, strongly suggests that the encoded proteins interact directly within the SPB. The nuclear envelope protein Mps2p (de la Cruz Munoz-Centeno *et al.*, 1999) was identified as an additional interactor of Bbp1p by the purification of a complex

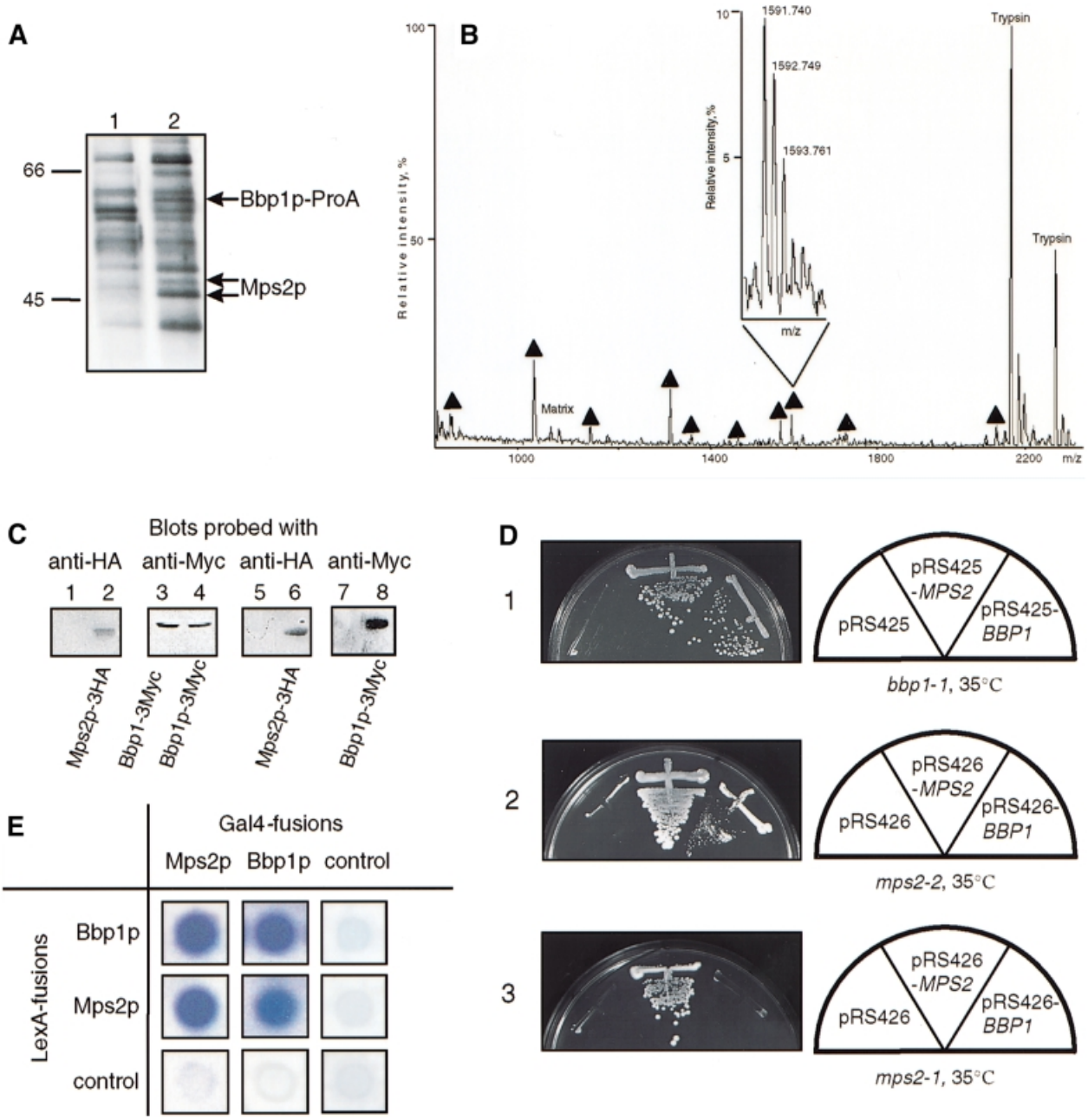

Fig. 6. Bbp1p interacts with Mps2p. (**A**) Purification of a complex containing ProA–Bbp1p. Lysates of wild-type (lane 1) and *BBP1-ProA* cells (lane 2) were incubated with IgG–Sepharose. The eluted proteins were analysed by SDS–PAGE and Coomassie Blue staining. (**B**) Identification of Bbp1p-interacting protein by MALDI peptide mapping. The mass spectrum acquired using 0.5 µl of the in gel digest of the 45 and 46 kDa bands revealed 10 peptide ions, which matched the calculated masses of protonated tryptic peptides originating from Mps2p with mass accuracy better than 75 p.p.m. (designated with filled triangles). These peptides covered ~30% of the sequence of Mps2p. Ions that originated from the HCCA matrix ('Matrix') and intensive ions of autolysis products of trypsin ('Trypsin') are also designated in the spectrum. The inset presents an isotopically resolved cluster of the peptide ion with *m/z* 1591.740 [mass resolution of the instrument was better than 6500 (full width at half-maximum)]. (**C**) Co-immunoprecipitation of Bbp1p and Mps2p. Lysates of cells (lanes 1–4) expressing *BBP1-3Myc MPS2* (lanes 1, 3, 5 and 7) or *BBP1-3Myc MPS2-3HA* (lanes 2, 4, 6 and 8) were either analysed directly by immunoblotting with the indicated antibodies (lanes 1–4) or incubated with anti-HA antibody beads (lanes 5–8). The precipitated proteins (lanes 5–8) were then analysed by immunoblotting with anti-Myc (lanes 7 and 8) or anti-HA antibodies (lanes 5 and 6). (**D**) High gene dosage suppression of *bbp1-1* by *MPS2* and of *mps2-2* by *BBP1*. (D-1) Cells of *bbp1-1* were unable to grow at 35°C with the control plasmid pRS425. Complementation was observed with *BBP1* on pRS425, whereas *MPS2* was identified as a high gene dosage suppressor. (D-2) Similarly, *mps2-2* cells with pRS426 were unable to grow at 35°C, however, grew with pRS426-*MPS2* or pRS426-*BBP1*. (D-3). In contrast, the temperature-dependent growth defect of *mps2-1* cells was not suppressed by pRS426-*BBP1*. (**E**) Two-hybrid interaction of Bbp1p and Mps2p. Blue colony colour indicates interaction.

containing Bbp1p–ProA, followed by matrix-assisted laser desorption/ionization (MALDI) analysis of the enriched proteins. The interaction of Bbp1p and Mps2p was confirmed by co-immunoprecipitation of the two proteins, the yeast two-hybrid system and by the high gene dosage suppression of the temperature-dependent growth defect of *bbp1-1* cells by *MPS2* and of *mps2-2* cells by *BBP1*. Finally, a direct binding of Mps2p with the C-terminal portion of Bbp1p was established by an *in vitro* binding experiment using the recombinant proteins.

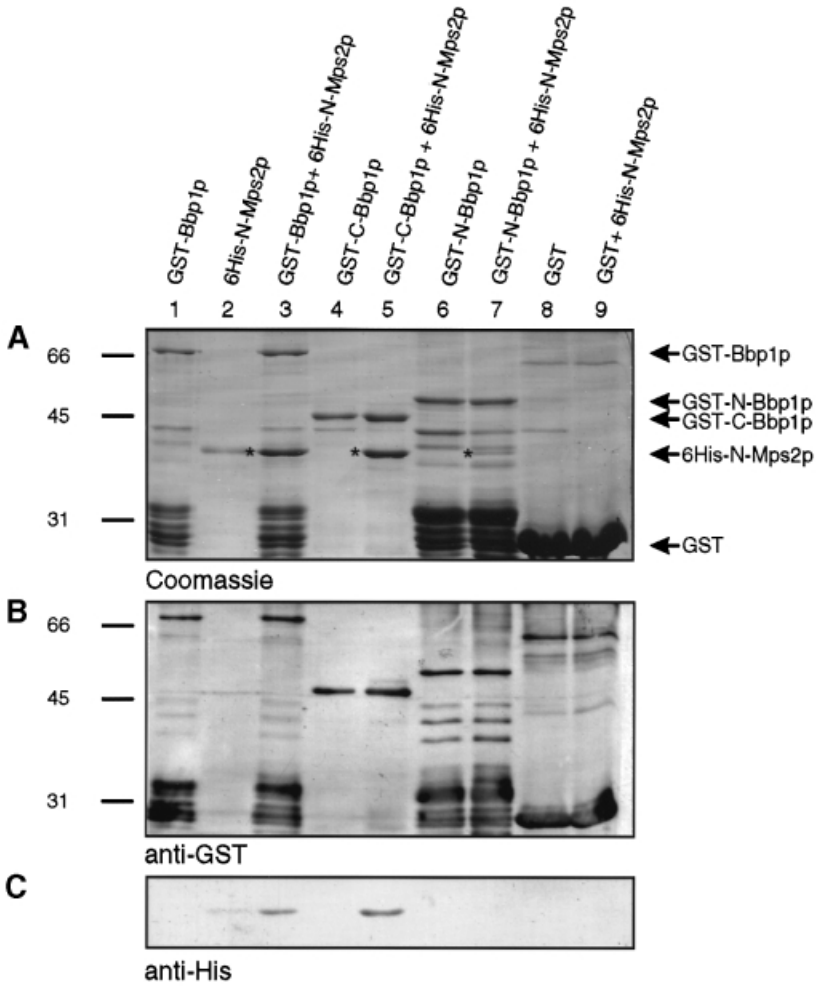

Fig. 7. Bbp1p binds directly to Mps2p. (**A**–**C**) GST–Bbp1p (lanes 1 and 3), GST–C-Bbp1p$^{202–385}$ (lanes 4 and 5), GST–N-Bbp1p$^{1–237}$ (lanes 6 and 7) and GST (lanes 8 and 9) bound to glutathione–Sepharose were incubated with (lanes 3, 5, 7 and 9) or without (lanes 1, 4, 6 and 8) purified His_6-N-Mps2p$^{1–307}$ (lane 2). The GST–Bbp1p derivatives and associated proteins were eluted with sample buffer. The eluate was analysed by Coomassie Blue staining (A) and by immunoblotting with anti-GST (B) or anti-His tag (C) antibodies. (A) Protein bands (lanes 2, 3, 5 and 7) corresponding in size to His_6-N-Mps2p$^{1–307}$ are marked by an asterisk.

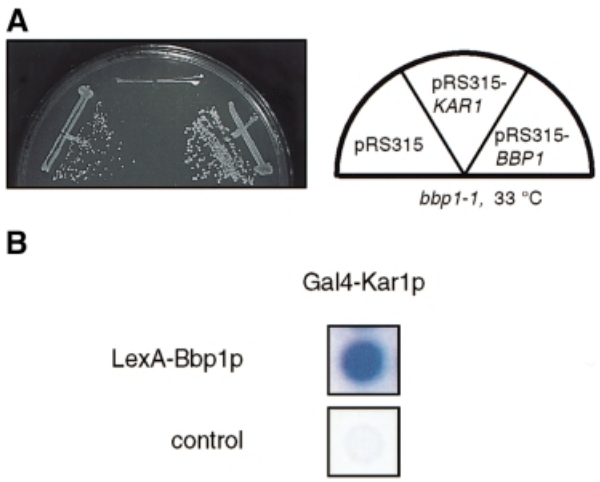

Fig. 8. *BBP1* interacts with *KAR1*. (**A**) *KAR1* increases the temperature-dependent growth defect of *bbp1-1* cells. Cells of *bbp1-1* carrying the control plasmid pRS315, *KAR1* or *BBP1* on pRS315 were incubated for 3 days at 33°C, a semi-permissive temperature of *bbp1-1* cells. (**B**) Kar1p interacts with Bbp1p in the yeast two-hybrid system. Blue colony colour indicates interaction.

Mps2p contains a single putative membrane-spanning segment from amino acids 311 to 327 and its N-terminal domain is predicted to be cytoplasmic (de la Cruz Munoz-Centeno *et al.*, 1999). Our *in vitro* binding experiment suggests that the cytoplasmic domain of Mps2p with a potential coiled-coil motif (amino acids 150–270) (de la Cruz Munoz-Centeno *et al.*, 1999) interacts with the C-terminal portion of Bbp1p, also containing a predicted coiled-coil region (amino acids 320–360) (Lupas *et al.*, 1991). If the coiled-coil domain of Mps2p confers binding to Bbp1p, we may expect that mutations in Mps2p, which affect the coiled-coil domain, reduce the interaction with Bbp1p, possibly resulting in a conditional lethal phenotype. Overexpression of *BBP1* may restore interaction, thereby suppressing the growth defect. Consistent with this, it was found that the temperature-dependent growth defect caused by the *mps2-2* (L191S) and *mps2-42* (I258V S259Y) mutations, but not by *mps2-1* (E39K), was suppressed by high dosage of *BBP1*. Importantly, only the E39K mutation is located outside the coiled-coil domain of Mps2p (de la Cruz Munoz-Centeno *et al.*, 1999).

An interaction of Bbp1p and Mps2p is also consistent with the observation that both proteins are associated with

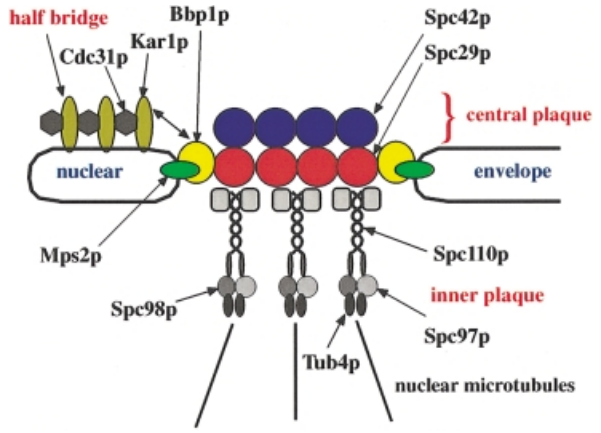

Fig. 9. Model for how the SPB is embedded in the nuclear envelope. Spc29p as a central plaque component (Adams and Kilmartin, 1999) connects Spc42p with the γ-tubulin complex binding protein Spc110p (Knop and Schiebel, 1997; Elliott *et al.*, 1999). In our model Bbp1p connects Spc29p with the nuclear envelope protein Mps2p (de la Cruz Munoz-Centeno *et al.*, 1999) at the central plaque periphery. Bbp1p also interacts with Kar1p, suggesting that it is involved in tethering the central plaque of the SPB to the half-bridge, containing Kar1p and Cdc31p (Spang *et al.*, 1993, 1995). Note that the outer plaque of the SPB is not shown.

the same SPB substructure. In the course of this study Bbp1p was localized by immunoelectron microscopy to the central plaque periphery of the SPB. A similar SPB localization has been determined for Mps2p (de la Cruz Munoz-Centeno *et al.*, 1999). However, it is important to note that we cannot exclude the possibility that a fraction of Bbp1p is also associated with other SPB substructures, e.g. throughout the central plaque. Such a localization may not have been detected due to the poor accessibility of this Bbp1p pool to the primary and secondary antibodies.

Our data are consistent with a model in which Spc29p binds to Bbp1p and Bbp1p binds to Mps2p (Figure 9). Since Spc29p interacts with Spc42p and Spc110p at the central plaque (Adams and Kilmartin, 1999; Elliott *et al.*, 1999) and Mps2p as an integral membrane protein is anchored in the nuclear envelope (de la Cruz Munoz-Centeno *et al.*, 1999), it is likely that the SPB is connected with the nuclear envelope via the interaction of the Bbp1p–Mps2p complex with Spc29p (Figure 9). However, in contrast to Spc29p, which spans the entire central plaque (Adams and Kilmartin, 1999), Mps2p and possibly Bbp1p are probably only associated with the central plaque periphery. This raises the possibility that the central plaque contains a specialized Spc29p rim that interacts with the Bbp1p–Mps2p complex. Furthermore, it is tempting to speculate that the Bbp1p–Mps2p complex attached to Spc29p represents the hook-like structure, which has been identified by high-voltage electron tomography of SPBs and that anchors the SPB in the nuclear envelope (O'Toole *et al.*, 1999).

The Bbp1p–Mps2p complex probably has a similar function during SPB duplication, namely in the insertion of the duplication plaque into the nuclear envelope. This notion is supported by the phenotype of the conditional lethal *mps2-1* (Winey *et al.*, 1991) and *bbp1-1* cells. Cells of *mps2-1* form a duplication plaque, which then fails to insert into the nuclear envelope and to assemble a nuclear inner plaque (Winey *et al.*, 1991). A similar phenotype was observed for *bbp1-1* cells. Electron microscopic studies revealed that *bbp1-1* cells enlarged their satellite into a duplication plaque with similar kinetics to wild-type cells. However, at a later time point *bbp1-1* cells still had not inserted the duplication plaque in the nuclear envelope, whereas wild-type cells had, suggesting that duplication plaque insertion is delayed or totally impaired in *bbp1-1* cells. It proved to be difficult to discriminate between these two possibilities by electron microscopy because only one SPB was observed in most *bbp1-1* cells after 1.25 h at 37°C, despite the appearance of two Spc72p SPB signals in the majority of *bbp1-1* cells as judged by indirect immunofluorescence. A likely explanation is that the newly formed SPB either partially disintegrates (Sundberg and Davis, 1997; Adams and Kilmartin, 1999) or is not recognized as such by electron microscopy because it appears similar to nuclear pores. However, the analysis of *bbp1-1* cells whose SPB was either marked with the nuclear Spc110p–GFP or the cytoplasmic Spc42p–GFP revealed that most of the newly formed SPBs of *bbp1-1* cells did not assemble an inner plaque. This deficiency is probably a direct consequence of the failure of *bbp1-1* cells to insert the duplication plaque into the nuclear envelope. Even when an inner plaque was assembled, this inner plaque organized only a few nuclear microtubules, which failed to become assembled into a functional spindle. Consequently, the newly formed SPB was unable to segregate the chromosomes, leaving the DNA associated with the functional SPB in the mother cell body.

We propose that during SPB duplication the Bbp1p–Mps2p complex interacts with the fraction of Spc29p that is associated with the satellite (Adams and Kilmartin, 1999) and the duplication plaque. This binding may become essential for the insertion of the duplication plaque into the nuclear envelope, followed by the assembly of the nuclear inner plaque.

Interaction of Bbp1p and Kar1p

Kar1p was identified as a further interactor of Bbp1p using the yeast two-hybrid system. Furthermore, an additional copy of *KAR1* increased the temperature-dependent growth defect of *bbp1-1* cells. Although attemps to co-immunoprecipitate Kar1p with Bbp1p failed (C.Schramm, unpublished), our data together with the finding that Bbp1p is localized close to the site where the half-bridge is attached to the central plaque make it likely that Bbp1p is involved in bridging the central plaque with the half-bridge (Figure 9). An important question is whether Bbp1p is only associated with the section of the outer plaque periphery that is in contact with the half-bridge. This is probably not the case, because in most SPB sections Bbp1p was detected at the central plaque periphery in the absence of a detectable half-bridge and, in addition, it was observed opposite to the site where the bridge was attached to the central plaque. Therefore, we assume that Bbp1p like Mps2p (de la Cruz Munoz-Centeno *et al.*, 1999) is distributed along the rim of the entire central plaque.

Materials and methods

General methods and materials, yeast strains and plasmids

Molecular weight markers used in all experiments were β-galactosidase (116 kDa), phosphorylase B (97 kDa), bovine serum albumin (BSA;

Table II. Yeast strains and plasmids used

Name	Genotype–construction	Source or reference
Yeast strains		
ESM401	*MATα ura3-52 his3Δ200 mps2-1*	Elliott *et al.* (1999)
ESM527	*MAT***a** *ura3-52 lys2-801 ade2-101 trp1Δ63 his3Δ200 leu2Δ1 spc29-2*	Elliott *et al.* (1999)
ESM578	*MAT***a** *ura3-52 lys2-801 ade2-101 trp1Δ63 his3Δ200 leu2Δ1 spc29-3*	Elliott *et al.* (1999)
ESM780	*MAT***a** *ura3-52 lys2-801 ade2-101 trp1Δ63 his3Δ200 leu2Δ1 Δmps2::HIS3MX4* pCS78	this study
ESM786	*MAT***a** *ura3-52 lys2-801 ade2-101 trp1Δ63 his3Δ200 leu2Δ1::*pSM733 *Δmps2::HIS3MX4*	this study
ESM787	*MAT***a** *ura3-52 lys2-801 ade2-101 trp1Δ63 his3Δ200 leu2Δ1::*pSM734 *Δmps2::HIS3MX4*	this study
SGY37	*MAT***a** *ura3-52::URA3-lexA-op-LacZ trp1 his3 leu2*	Geissler *et al.* (1996)
YAS8	*MAT***a** *ura3-52 lys2-801 ade2-101 trp1Δ63 his3Δ200 leu2Δ1 Δsst1::URA3*	Spang *et al.* (1995)
YCS4	*MAT***a** *ura3-52 lys2-801 ade2-101 trp1Δ63 his3Δ200 leu2Δ1 BBP1-ProA-kanMX6*	this study
YCS5	*MAT***a** *ura3-52 lys2-801 ade2-101 trp1Δ63 his3Δ200 leu2Δ1 BBP1-3Myc-kanMX6*	this study
YCS17	*MAT***a** *ura3-52 lys2-801 ade2-101 trp1Δ63 his3Δ200 leu2Δ1 Δbbp1::HIS3MX4* pCS16	this study
YCS64	*MAT***a** *ura3-52 lys2-801 ade2-101 trp1Δ63::*pCS51 *his3Δ200 leu2Δ1 Δbbp1::HIS3MX4*	this study
YCS66	*MAT***a** *ura3-52 lys2-801 ade2-101 trp1Δ63::*pCS53 *his3Δ200 leu2Δ1 Δbbp1::HIS3MX4*	this study
YCS70	*MAT***a** *ura3-52 lys2-801 ade2-101 trp1Δ63::*pCS51 *his3Δ200 leu2Δ1 Δbbp1::HIS3MX4 Δsst1::URA3*	this study
YCS72	*MAT***a** *ura3-52 lys2-801 ade2-101 trp1Δ63::*pCS53 *his3Δ200 leu2Δ1 Δbbp1::HIS3MX4 Δsst1::URA3*	this study
YCS84	*MAT***a** *ura3-52 lys2-801 ade2-101 trp1Δ63 his3Δ200 leu2Δ1 BBP1-3Myc-kanMX6 MPS2-3HA-HIS3MX6*	this study
YCS109	*MAT***a** *ura3-52 lys2-801 ade2-101 trp1Δ63::*pCS51 *his3Δ200 leu2Δ1 Δbbp1::HIS3MX4* pSM740	this study
YCS110	*MAT***a** *ura3-52 lys2-801 ade2-101 trp1Δ63::*pCS51 *his3Δ200 leu2Δ1 Δbbp1::HIS3MX4* pSM782	this study
YPH499	*MAT***a** *ura3-52 lys2-801 ade2-101 trp1Δ63 his3Δ200 leu2Δ1*	Sikorski and Hieter (1989)
Plasmids		
pAL002[a]	pET28c containing $MPS2^{1–307}$	this study
pCS1	pGEX-5X-1 containing *BBP1*	this study
pCS7	pGEX-5X-1 containing $BBP1^{1–237}$	this study
pCS8	pGEX-5X-1 containing $BBP1^{202–385}$	this study
pCS14	pRS425 containing *BBP1*	this study
pCS15	pRS315 containing *BBP1*	this study
pCS16	pRS316 containing *BBP1*	this study
pCS51	pRS304 containing *bbp1-1*	this study
pCS53	pRS304 containing *bbp1-2*	this study
pCS71	pRS315 containing *MPS2*	this study
pCS72	pRS425 containing *MPS2*	this study
pCS78	pRS316 containing *MPS2*	this study
pET28c	*E.coli* expression vector containing His_6 under control of the T7 promotor	Novagen
pGEX-5X-1	*E.coli* expression vector containing GST under control of the lacZ promotor	Pharmacia
pMM5	two-hybrid vector: pRS423 containing *Gal1-LexA-Myc*	M.Knop
pMM6	two-hybrid vector: pRS425 containing *Gal1-GAL4-HA*	M.Knop
pRS304	*TRP1*-based yeast integration vector	Sikorski and Hieter (1989)
pRS305	*LEU2*-based yeast integration vector	Sikorski and Hieter (1989)
pRS315	*CEN6*, *LEU2*-based yeast-*E.coli* shuttle vector	Sikorski and Hieter (1989)
pRS316	*CEN6*, *URA3*-based yeast-*E.coli* shuttle vector	Sikorski and Hieter (1989)
pRS423	2 μm, *HIS3*-based yeast-*E.coli* shuttle vector	Christianson *et al.* (1992)
pRS425	2 μm, *LEU2*-based yeast-*E.coli* shuttle vector	Christianson *et al.* (1992)
pRS426	2 μm, *URA3*-based yeast-*E.coli* shuttle vector	Christianson *et al.* (1992)
pSE3	pRS425 containing *SPC29*	Elliott *et al.* (1999)
pSE41	pET28c containing *SPC29*	this study
pSE63	pMM5 containing *SPC29*	this study
pSE64	pMM6 containing *SPC29*	this study
pSE65	pMM5 containing *BBP1*	this study
pSE66	pMM6 containing *BBP1*	this study
pSE67	pMM5 containing $MPS2^{1–307}$	this study
pSE68	pMM6 containing $MPS2^{1–307}$	this study
pSE71	pMM5 containing $KAR1^{1–408}$	this study
pSE72	pMM6 containing $KAR1^{1–408}$	this study
pSM30	pRS315 containing *KAR1*	Spang *et al.* (1995)
pSM56	pRS426 containing *CDC31*	Geier *et al.* (1996)
pSM119	pRS315 containing *KAR1*	Spang *et al.* (1995)
pSM567	pRS426 containing *SPC29*	this study
pSM733	pRS305 containing *mps2-2*	this study
pSM734	pRS305 containing *mps2-42*	this study
pSM740	pRS315 containing *SPC42-GFP-kanMX6*	this study
pSM743	pRS426 containing *MPS2*	this study
pSM751	pRS426 containing *BBP1*	this study
pSM782	pRS315 containing *SPC110-GFP-kanMX6*	this study
pSM794	pRS316 containing *NDC1*	this study
pSM795	pRS315 containing *NDC1*	this study

[a]$MPS2^{1–307}$ indicates that codons 1–307 of *MPS2* have been cloned into plasmid pET28c.

66 kDa), ovalbumin (45 kDa), carbonic anhydrase (31 kDa) and trypsin inhibitor (21.5 kDa). Strains and plasmids are listed in Table II. Yeast strains used in this study were derivatives of strain S228c; they were constructed using PCR-amplified cassettes (Wach *et al.*, 1997; Knop *et al.*, 1999). *BBP1* and *MPS2* were mutagenized by PCR and conditional lethal alleles were selected as described (Muhlrad *et al.*, 1992). *bbp1-1* carries multiple missense mutations resulting in N97S, H135R, N234D and D243E, whereas the mutations in *bbp1-2* caused T66P, S106N and M230S exchanges. The mutations in *mps2-2* resulted in I258V S259Y and in *mps2-42* in L191S. *bbp1-1*, *bbp1-2*, *mps2-2* and *mps2-42* on the integration plasmids pRS304 or pRS305 were integrated into the *TRP1* or *LEU2* locus of yeast strains YCS17 or ESM780, respectively. The transformants were grown at 23°C on 5-fluoroorotic acid (5-FOA) plates, which select against the *URA3*-based pRS316 plasmids. *MPS2* was cloned by gap repair. *BBP1* was subcloned from plasmid YEp13-42.3.

Suppression of spc29-2, bbp1-1 or mps2-2 cells

High gene dosage suppressors of *spc29-2* cells were selected as described (Geissler *et al*., 1996). Two of the suppressing plasmids (YEp13-10.1, 42.3) contained *BBP1*. *BBP1* subcloned into the 2 μm plasmid pRS425 suppressed the temperature-dependent growth defect of *spc29-2* cells. Additional plasmids that suppressed *spc29-2* carried *CDC31* (YEp13-12.7 and 15.3).

Cells of *bbp1-1*, *bbp1-2* and *mps2-2* were transformed with 2 μm plasmids pRS425 or pRS426 carrying *BBP1*, *CDC31*, *MPS2* and *SPC29*. *KAR1* and *NDC1* were on the centromere-based plasmids pRS315 or pRS316 because they are toxic for wild-type cells on 2 μm plasmids (Rose and Fink, 1987; Chial *et al.*, 1999). The transformants were tested for growth at 35 and 37°C on selective plates.

Two-hybrid interactions

Gene fusions were made using plasmid pMM5, which expresses the LexA gene fusion under the control of the *Gal1* promoter in pRS423. Plasmid pMM6 was chosen as the activation domain vector. It contains the *GAL4* fragment of pACT2 (Durfee *et al.*, 1993) under the control of the *Gal1* promoter in pRS425. Derivatives of these plasmids were transformed into yeast strain SGY37 bearing a *lexA–operator–lacZ* reporter construct. Transformants were grown on nitrocellulose filters placed onto SC agar with 2% glucose lacking leucine and histidine for 2 days at 30°C. The filters were then placed on SC agar with 2% galactose, 2% raffinose, but lacking leucine and histidine, for 12 h at 30°C. β-galactosidase activity was determined by overlaying the nitrocellulose filter with 0.5 M potassium phosphate-buffered (pH 7.0) top agar containing 0.1% SDS, 6% dimethylformamide (DMF) and 120 μg/ml 5-bromo-4-chloro-3-indoyl-β-D-galactoside (X-Gal).

Anti-Bbp1p antibodies

BBP1 was subcloned into *Escherichia coli* expression vector pGEX-5X-1 (Pharmacia). The GST–Bbp1p fusion protein was expressed in *E.coli* BL21 DE3 (Studier and Moffat, 1986) and purified using glutathione–Sepharose. Antibodies against the purified protein were raised in rabbits using standard procedures. These antibodies were affinity purified using GST–Bbp1p coupled to CNBr-activated Sepharose (Pharmacia) with GST coupled to Sepharose as a pre-column.

Synchronization of yeast cells and flow cytometry

Yeast cells were synchronized with 1 μg/ml (Δ*sst1* cells) or 10 μg/ml (*SST1*) synthetic α-factor for 2 h at 23°C until most (>95%) of the cells were arrested in the G_1 phase of the cell cycle. Cells were prepared for flow cytometry as described (Hutter and Eipel, 1979).

Electron microscopy and immunoelectron microscopy

Electron microscopy of yeast cells was performed according to Byers and Goetsch (1991). Nuclei and SPBs were enriched from strain YPH499 (Rout and Kilmartin, 1990). Immunoelectron microscopy of yeast cells and nuclei was performed with either anti-Bbp1p or anti-Myc antibodies (*BBP1-3Myc* cells). Cells were then incubated with Fab fragments of goat anti-rabbit IgGs or goat anti-mouse IgGs coupled to ultrasmall gold particles (Nano Probes) (Knop *et al.*, 1997). The ultrasmall gold particles were then silver enhanced (Danscher, 1981). SPBs were spun onto a coverslip (20 000 *g*, 30 min, 4°C), which was then blocked with BSA. The coverslip was incubated with anti-Bbp1p antibodies, washed with phosphate-buffered saline (PBS)–BSA and then incubated with goat anti-rabbit IgGs conjugated with 12 nm gold particles (Nano Probes). The washed coverslips were overlaid with spurr resin in a gelatin capsule. The spurr resin was allowed to polymerize at 65°C for 8 h. The sections were contrasted with 2% uranyl acetate in 70% methanol and lead citrate for 5 min at 20°C in the dark.

Affinity purification of Bbp1p–ProA

Cells (50 g) of a *BBP1-ProA* strain were lysed with glass beads in L-buffer (50 mM Tris–HCl pH 7.6, 10 mM EDTA, 1 mM EGTA, 100 mM NaCl, 5% glycerol). The lysate was then incubated with 1% Triton X-100 for 20 min at 4°C. The insoluble material was removed by centrifugation (15 min at 12 000 *g*). The supernatant containing Bbp1p–ProA was applied to an IgG–Sepharose column. The column was washed as described (Knop and Schiebel, 1997). Proteins were eluted with 0.5 M ammonium acetate pH 3.5. The lyophilized proteins were washed once with water and finally dissolved in sample buffer. Proteins were separated by SDS–PAGE using a gradient gel and then analysed by MALDI analysis (Shevchenko *et al.*, 1996).

GFP fluorescence, immunofluorescence and immunoprecipitation

SPC110-GFP and *SPC42-GFP* were cloned by gap repair using yeast strains with chromosomally integrated *SPC110-GFP-kanMX6* and *SPC42-GFP-kanMX6*. *bbp1-1* cells with *SPC110-GFP-kanMX6* or *SPC42-GFP-kanMX6* plasmids were analysed by fluorescence microscopy after fixation of cells with phosphate-buffered (150 mM potassium phosphate pH 6.5) 6% paraformaldehyde for 10 min at 20°C.

Indirect immunofluorescence of yeast cells was performed using published protocols (Kilmartin and Adams, 1984; Rout and Kilmartin, 1990). Microtubules were detected with the mouse monoclonal antibody WA3 (Spang *et al.*, 1996). Affinity-purified rabbit anti-Spc72p antibodies were used to detect Spc72p (Knop and Schiebel, 1998). Proteins were immunoprecipitated with mouse monoclonal anti-HA (12CA5) antibody coupled to protein A–Sepharose (Geissler *et al.*, 1996; Knop and Schiebel, 1998). Anti-HA antibodies were from Hiss Diagnostics. The precipitate was analysed by immunoblotting with anti-Myc (9E10; Boehringer Mannheim) and anti-HA antibodies. Mouse monoclonal anti-His tag antibodies were from Dianova.

In vitro binding of Bbp1p to Mps2p and of Spc29p to Bbp1p

His_6-$MPS2^{1–307}$ in pET28c was expressed and purified from *E.coli* BL21 DE3 pLysS (Studier and Moffat, 1986). Bbp1p–GST fusion proteins or GST were bound to glutathione–Sepharose and the purified His_6-$Mps2p^{1–307}$ was incubated with the glutathione beads for 1 h at 4°C in PBS containing 0.1% Triton X-100. The resin was washed once with PBS, 0.1% Triton X-100, followed by two washes with PBS. Bound proteins were eluted with SDS–sample buffer and analysed by Coomassie Blue staining and immunoblotting with anti-His tag and anti-Bbp1p antibodies.

SPC29 in plasmid pET28c was translated in the presence of [^{35}S]methionine using an *in vitro* transcription/translation system (Promega). The [^{35}S]Spc29p was incubated with purified GST or GST–Bbp1p for 1 h at 4°C in PBS containing 0.1% Triton X-100. The washed beads were heated with sample buffer and the eluted proteins were analysed by autoradiography and immunoblotting using anti-Bbp1p antibodies.

Acknowledgements

We thank Dr M.Knop for the pMM5 and pMM6 plasmids, and Dr M.Winey for the *mps2-1* mutant and plasmid pRS426-*NDC1*. M.O'Prey is acknowledged for thin serial sections of embedded samples for electron microscopy, and M.Mullin and E.Robertson for help with the electron microscope. We are very grateful to Dr A.Camasses for the construction of *mps2(ts)* alleles. This work was carried out with support from the Cancer Research Campaign.

References

Adams,I.R. and Kilmartin,J.V. (1999) Localization of core spindle pole body (SPB) components during SPB duplication in *Saccharomyces cerevisiae*. *J. Cell Biol.*, **145**, 809–823.

Baum,P., Furlong,C. and Byers,B. (1986) Yeast gene required for spindle pole body duplication: homology of its product with Ca^{2+}-binding proteins. *Proc. Natl Acad. Sci. USA*, **83**, 5512–5516.

Biggins,S. and Rose,M.D. (1994) Direct interaction between yeast spindle pole body components: Kar1p is required for Cdc31p localization to the spindle pole body. *J. Cell Biol.*, **125**, 843–852.

Biggins,S., Ivanovska,I. and Rose,M.D. (1996) Yeast ubiquitin like genes are involved in duplication of the microtubule organizing center. *J. Cell Biol.*, **133**, 1331–1346.

Brachat,A., Kilmartin,J.V., Wach,A. and Philippsen,P. (1998) *Saccharomyces cerevisiae* cells with defective spindle pole body outer plaques accomplish nuclear migration via half-bridge-organized microtubules. *Mol. Biol. Cell*, **9**, 977–991.

Bullitt,E., Rout,M.P., Kilmartin,J.V. and Akey,C.W. (1997) The yeast spindle pole body is assembled around a central crystal of Spc42p. *Cell*, **89**, 1077–1086.

Byers,B. and Goetsch,L. (1975) Behavior of spindles and spindle plaques in the cell cycle and conjugation of *Saccharomyces cerevisiae*. *J. Bacteriol.*, **124**, 511–523.

Byers,B. and Goetsch,L. (1991) Preparation of yeast cells for thin-section electron microscopy. *Methods Enzymol.*, **194**, 602–608.

Chial,H.J., Rout,M.P., Giddings,T.H. and Winey,M. (1998) *Saccharomyces cerevisiae* Ndc1p is a shared component of nuclear pore complexes and spindle pole bodies. *J. Cell Biol.*, **143**, 1789–1800.

Chial,H.J., Giddings,T.H., Siewert,E.A., Hoyt,M.A. and Winey,M. (1999) Altered dosage of the *Saccharomyces cerevisiae* spindle pole body duplication gene, *NDC1*, leads to aneuploidy and polyploidy. *Proc. Natl Acad. Sci. USA*, **96**, 10200–10205.

Christianson,T.W., Sikorski,R.S., Dante,M., Shero,J.H. and Hieter,P. (1992) Multifunctional yeast high-copy-number shuttle vectors. *Gene*, **110**, 119–122.

Danscher,G. (1981) Localization of gold in biological tissue. A photochemical method for light and electron microscopy. *Histochemistry*, **71**, 81–88.

de la Cruz Munoz-Centeno,M., McBratney,S., Monterrosa,A., Byers,B., Mann,C. and Winey,M. (1999) *Saccharomyces cerevisiae MPS2* encodes a membrane protein localized at the spindle pole body and the nuclear envelope. *Mol. Biol. Cell*, **10**, 2393–2406.

Durfee,T., Becherer,K., Chen,P.L., Yeh,S.H., Yang,Y., Kilburn,A.E., Lee,W.H. and Elledge,S.J. (1993) The retinoblastoma protein associates with the protein phosphatase type 1 catalytic subunit. *Genes Dev.*, **7**, 555–569.

Elliott,S., Knop,M., Schlenstedt,G. and Schiebel,E. (1999) Spc29p is a component of the Spc110p-subcomplex and is essential for spindle pole body duplication. *Proc. Natl Acad. Sci. USA*, **96**, 6205–6210.

Geissler,S., Pereira,G., Spang,A., Knop,M., Souès,S., Kilmartin,J. and Schiebel,E. (1996) The spindle pole body component Spc98p interacts with the γ-tubulin-like Tub4p of *Saccharomyces cerevisiae* at the sites of microtubule attachment. *EMBO J.*, **15**, 3899–3911.

Hutter,K.J. and Eipel,H.E. (1979) Microbial determination by flow cytometry. *J. Gen. Microbiol.*, **113**, 369–375.

Kilmartin,J.V. and Adams,A.E.M. (1984) Structural rearrangements of tubulin and actin during the cell cycle of the yeast *Saccharomyces cerevisiae*. *J. Cell Biol.*, **98**, 922–933.

Kilmartin,J.V. and Goh,P.Y. (1996) Spc110p: assembly properties and role in the connection of nuclear microtubules to the yeast spindle pole body. *EMBO J.*, **15**, 4592–4602.

Knop,M. and Schiebel,E. (1997) Spc98p and Spc97p of the yeast γ-tubulin complex mediate binding to the spindle pole body via their interaction with Spc110p. *EMBO J.*, **16**, 6985–6995.

Knop,M. and Schiebel,E. (1998) Receptors determine the cellular localization of a γ-tubulin complex and thereby the site of microtubule formation. *EMBO J.*, **17**, 3952–3967.

Knop,M., Pereira,G., Geissler,S., Grein,K. and Schiebel,E. (1997) The spindle pole body component Spc97p interacts with the γ-tubulin of *Saccharomyces cerevisiae* and functions in microtubule organization and spindle pole body duplication. *EMBO J.*, **16**, 1550–1564.

Knop,M., Siegers,K., Pereira,G., Zachariae,W., Winsor,B., Nasmyth,K. and Schiebel,E. (1999) Epitope tagging of yeast genes using a PCR-based strategy: more tags and improved practical routines. *Yeast*, **15**, 963–972.

Lauzé,E., Stoelcker,B., Luca,F.C., Weiss,E., Schutz,A.R. and Winey,M. (1995) Yeast spindle pole body duplication gene *MPS1* encodes an essential dual specificity protein kinase. *EMBO J.*, **14**, 1655–1663.

Lupas,A., Van Dyke,M. and Stock,J. (1991) Predicting coiled coils from protein sequences. *Science*, **252**, 1162–1164.

Muhlrad,D., Hunter,R. and Parker,R. (1992) A rapid method for localized mutagenesis of yeast genes. *Yeast*, **8**, 79–82.

O'Toole,E.T., Winey,M. and McIntosh,J.R. (1999) High-voltage electron tomography of spindle pole bodies and early mitotic spindles in the yeast *Saccharomyces cerevisiae*. *Mol. Biol. Cell*, **10**, 2017–2031.

Pereira,G., Knop,M. and Schiebel,E. (1998) Spc98p directs the yeast γ-tubulin complex into the nucleus and is subject to cell cycle-dependent phosphorylation on the nuclear side of the spindle pole body. *Mol. Biol. Cell*, **9**, 775–793.

Pereira,G., Grueneberg,U., Knop,M. and Schiebel,E. (1999) Interaction of the yeast γ-tubulin complex binding protein Spc72p with Kar1p is essential for microtubule function during karyogamy. *EMBO J.*, **18**, 4180–4196.

Rose,M.D. and Fink,G.R. (1987) *KAR1*, a gene required for function of both intranuclear and extranuclear microtubules in yeast. *Cell*, **48**, 1047–1060.

Rout,M.P. and Kilmartin,J.V. (1990) Components of the yeast spindle and spindle pole body. *J. Cell Biol.*, **111**, 1913–1927.

Shevchenko,A., Jensen,O.N., Podtelejnikov,A.V., Sagliocco,F., Wilm,M., Vorm,O., Mortensen,P., Boucherie,H. and Mann,M. (1996) Linking genome and proteome by mass spectrometry: large scale identification of yeast proteins from two dimensional gels. *Proc. Natl Acad. Sci. USA*, **93**, 14440–14445.

Sikorski,R.S. and Hieter,P. (1989) A system of shuttle vectors and yeast host strains designed for efficient manipulation of DNA in *Saccharomyces cerevisiae*. *Genetics*, **122**, 19–27.

Spang,A., Courtney,I., Fackler,U., Matzner,M. and Schiebel,E. (1993) The calcium-binding protein cell division cycle 31 of *Saccharomyces cerevisiae* is a component of the half bridge of the spindle pole body. *J. Cell Biol.*, **123**, 405–416.

Spang,A., Courtney,I., Grein,K., Matzner,M. and Schiebel,E. (1995) The Cdc31p-binding protein Kar1p is a component of the half bridge of the yeast spindle pole body. *J. Cell Biol.*, **128**, 863–877.

Spang,A., Geissler,S., Grein,K. and Schiebel,E. (1996) γ-Tubulin-like Tub4p of *Saccharomyces cerevisiae* is associated with the spindle pole body substructures that organize microtubules and is required for mitotic spindle formation. *J. Cell Biol.*, **134**, 429–441.

Studier,F.W. and Moffat,B.A. (1986) Use of bacteriophage T7 RNA polymerase to direct selective high level expression of cloned genes. *J. Mol. Biol.*, **189**, 113–130.

Sundberg,H.A. and Davis,T.A. (1997) A mutational analysis identifies three functional regions of the spindle pole body component Spc110p in *Saccharomyces cerevisiae*. *Mol. Biol. Cell*, **8**, 2575–2590.

Vallen,E.A., Hiller,M.A., Scherson,T.Y. and Rose,M.D. (1992) Separate domains of *KAR1* mediate distinct functions in mitosis and nuclear fusion. *J. Cell Biol.*, **117**, 1277–1287.

Vallen,E.A., Ho,W., Winey,M. and Rose,M.D. (1994) Genetic interactions between *CDC31* and *KAR1*, two genes required for duplication of the microtubule organizing center in *Saccharomyces cerevisiae*. *Genetics*, **137**, 407–422.

Wach,A., Brachat,A., Alberti-Segui,C., Rebischung,C. and Philippsen,P. (1997) Heterologous *HIS3* marker and *GFP* reporter modules for PCR-targeting in *Saccharomyces cerevisiae*. *Yeast*, **13**, 1065–1075.

Weiss,E. and Winey,M. (1996) The *Saccharomyces cerevisiae* spindle pole body duplication gene *MPS1* is part of a mitotic checkpoint. *J. Cell Biol.*, **132**, 111–123.

Wigge,P.A., Jensen,O.N., Holmes,S., Souès,S., Mann,M. and Kilmartin,J.V. (1998) Analysis of the *Saccharomyces* spindle pole by matrix-assisted laser desorption/ionization (MALDI) mass spectrometry. *J. Cell Biol.*, **141**, 967–977.

Winey,M., Goetsch,L., Baum,P. and Byers,B. (1991) *MPS1* and *MPS2*: novel yeast genes defining distinct steps of spindle pole body duplication. *J. Cell Biol.*, **114**, 745–754.

Winey,M., Hoyt,M.A., Chan,C., Goetsch,L., Botstein,D. and Byers,B. (1993) *NDC1*: a nuclear periphery component required for yeast spindle pole body duplication. *J. Cell Biol.*, **122**, 743–751.

Received October 14, 1999; revised November 23, 1999; accepted November 25, 1999